Contents

Chapter 1

Prospects for Neutral MSSM Higgs Search Improvement

The neutral MSSM Higgs boson search, described in the previous chapter, suffers strongly of poor b-tagging performance due to the particular phase space required, this bound the potential of this search, improving b-tagging would result in a major improvement of the search sensitivity. This chapter investigates an alternative to the commonly used calorimeter jets in ATLAS, which is trackjets b-tagging. The prospects for successfully use trackjets b-tagging in the future neutral MSSM Higgs boson search are reported, b-tagging on trackjets was never attempted before. In section 1.1 an introduction to the b-tagging challenges of the analysis and to trackjets is given. Section 1.2 presents trackjets performance on b-tagging in comparison with calorimeter jets, preliminary results on the impact of trackjets to the analysis are also described here. Finally, in section 1.3 an evaluation of trackjets systematic uncertainties is presented.

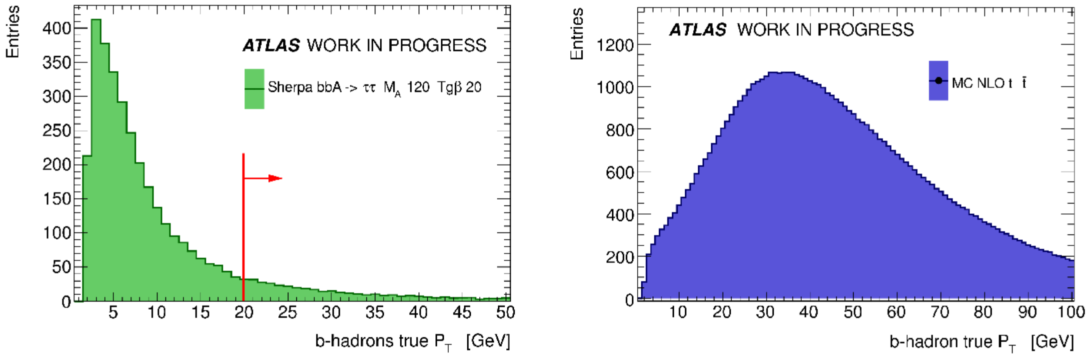

Figure 1.1: Comparison of simulated b-hadron distribution for signal b-associated production events (left) and $t\bar{t}$ events (right). The red line in the figure shows the acceptance region due to calibrated jet P_T requirements.

1.1 Introduction to Trackjets

The neutral MSSM Higgs search, as described in chapter **??**, splits the dataset in two category by means of the presence or the absence of a b-tagged jet, the b-tagged category is optimized for the b-associated production mechanism, in which the Higgs is produced in association with two b-jets. Figure 1.1 shows a comparison between the P_T spectrum of simulated b-hadron in $bb/A/h/H$ production and $t\bar{t}$ events, the signal prefers b-hadron with relatively low transverse momentum, which is actually the major challenge for the b-tag category. Due to the high amount of pileup and ambient energy density in the events, calorimeter jets are not calibrated below 20 GeV in P_T (see chapter **??**), systematic uncertainties and performance are also not evaluated below this threshold, this means that, currently, the low transverse momentum phase space is not accessible to canonical calorimeter jets (*calojets* in the following). Calojets are then inconvenient for $bb/A/h/H$ production and one of the major reason for sensitivity lost in the b-tag category. Another challenge to this search is the drop in b-tagging performance at low transverse momentum, the MV1 tagger (see chapter **??**) efficiency , in fact, decreases rapidly with jet P_T, reaching a minimum of 50% at 20 GeV [84, 85] (using the tagging point with 70% efficiency).

A solution to access jets with low transverse momentum in to use *trackjets* instead of calojets. Trackjets are anti-kt jets (see chapter**??**) reconstructed by clustering inner detector tracks, for them it is possible to take advantage of the tracks longitudinal (z) impact parameter information and build trackjets in three dimensions $\eta - \phi - z$. Trackjets will then contains only tracks originating from the same interaction point (reconstructed vertex), this feature make them very robust with respect to pileup. B-tagging has never been tested before on trackjets, in section 1.2 the first study of b-tagging over trackjets performances is reported.

Trackjets are builded in the ATLAS reconstruction software by the *TrackZTool*, this runs the anti-kt clustering algorithm on a subset of tracks which can be defined by the user. For the purposes of this thesis trackjets are reconstructed out of tracks that passes the following quality selection criteria:

- $|z_{track} - z_{PV}| < 2$ mm, The track should be associated to the primary vertex (PV).
- $|z_{PV} * sin(\theta)| < 1.5$ mm, which is a measure of how much the track is pointing to the PV in the plane that contain the beam axis.
- $d_{PV} < 1.5$ mm, where d_{PV} is the distance of minimum approach of the track to the primary vertex in the plane orthogonal to the beam axis.
- At least one pixel hit and at least 6 SCT hits (including SCT holes).
- At least one b-layer hit if expected (i.e. the module passed by the track was active).
- $|\eta| < 2.5$
- $P_T > 300$ MeV
- To build a trackjets is necessary to cluster at least two tracks
- A trackjet is produced and stored if the sum of its tracks has $P_T > 2$ GeV.

it has been shown that those selections, together with a maximum cone size for clustering of $\Delta R = 0.6$, are the best compromise between quality requirements, aimed to control fake tracks, and b-hadron reconstruction efficiency. Several MC simulation samples has been produced with the purpose of studying trackjets performance,

Process	MC Generator	Purpose
Minimum bias	Pythia	Systematics study
$b\bar{b}$	Alpgen	Performance for low P_T b-tagging
$Z \to \tau\tau$	Pythia	Impact on the MSSM Higgs search
$t\bar{t}$	MC@NLO	Impact on the MSSM Higgs search
MSSM $bb/A/h/H$	Sherpa	Impact on the MSSM Higgs search

Table 1.1: Monte Carlo simulation sample produced for the studies reported in this chapter.

trackjets were reconstructed and b-tagged using an ad-hoc implementation of the TrackZTool within the ATLAS software framework, table 1.1 reports a summary of the produced samples along with their usage in this thesis.

1.2 Trackjet Performance

Many analysis could profit from an enhanced b-jet reconstruction efficiency at low P_T, the studies presented in this section are aimed to compare performance of common b-tagging algorithm and b-jet reconstruction efficiency between calojets and trackjets, these studies are specially focused on low transverse momentum.

Despite trackjets are more robust with respect to pileup, which makes them appealing, they can only reconstruct the charged part of the jet, the neutral part is lost. According to isospin invariance the expected charged fraction in a jet is roughly 2/3 of the total, the trackjet momentum will be then shifted and its direction will have a larger uncertainty. Figure 1.2 shows a comparison of trackjet and calojet transverse momentum residuals with respect to *truthjet* P_T (reconstructed jets from truth particle), here truthjet are matched with jets within a ΔR cone of 0.4 (jet splitting effect are resolved by matching with the nearest jet). The trackjets energy shift may be critical for b-tagging algorithm since some of them strongly rely on the measurement of jet axis and jet P_T.

To compare performance of trackjet and calojet an anti-kt cone size of $\Delta R = 0.4$ is chosen, if a reconstructed jets lies within $\Delta R < 0.3$ from a simulated b-hadron

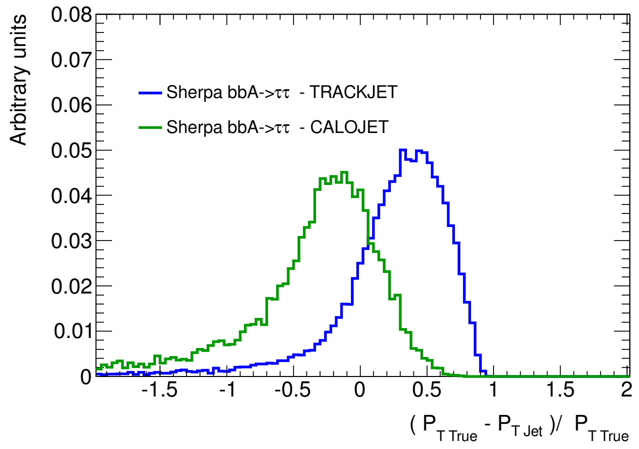

Figure 1.2: Residuals comparison of trackjet and calojet P_T with respect simulated jet P_T.

in the event, this jet is said to *match* with a b-hadron. *Reconstruction efficiency* is then defined as the ratio between the number of matched b-hadron and the total number of b-hadron within inner detector acceptance. Figure 1.3 compare b-hadron reconstruction efficiency between calojet and trackjets, the latter shows a higher reconstruction efficiency for low transverse momentum due to their robustness to pileup.

1.2.1 B-tagging on Trackjets

Performance of b-tagging algorithms are usually described by means of tagging efficiency and rejection power. The *tagging efficiency* is the fraction of matched jets which passes a determined selection on a tagging algorithm, i.e. which are *tagged*. The *rejection* is the inverse of the misidentifying rate, i.e. the inverse of the fraction of the jets which are not matched with a b-hadron or c-hadron, but are tagged. Fixing the selection value for a given tagging algorithm will fix a point in the efficiency-rejection plane, this is a convenient way to compare performance of b-tagging algorithms and is shown in figure 1.4 for trackjets. Figure 1.5 instead shows the rejection as a function of trackjets P_T for the tagging point which gives 50% tagging efficiency. Mistagging rate is rapidly increasing for low transverse momentum trackjets, revealing the necessity of a dedicated tagging algorithm for

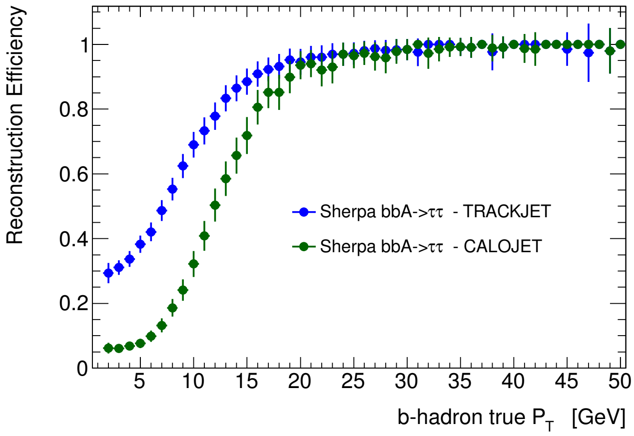

Figure 1.3: Comparison of b-hadron reconstruction efficiency for trackjet and calojet as a function of the simulated b-hadron P_T. Note that calojet and trackjet have a requirement at reconstruction level to be respectively with $P_T > 7$ and 2 GeV, a fair comparison in this plot is only possible above 10 GeV in P_T.

low P_T jets.

The previously introduced rejection and tagging efficiency do not allow a fair comparison between trackjets and calojets, the latter, in fact, can be reconstructed also in case no tracks are associated with them, in this case any tagging algorithm would likely fail altering the rejection distribution. It is convenient to use instead the following quantities: *effective rejection*, which is the inverse of the number of mistagged jets per event, and the b-hadron reconstruction efficiency, which is defined above. Figure 1.6 shows a comparison between calojets and trackjets for the two variables just defined, for a given b-hadron reconstruction efficiency trackjets can achieve higher rejection, which is quite promising. For a fair comparison with calojets, trackjets in figure 1.6 are selected in the transverse momentum range between 4 and 33 GeV, while calojets between 8 and 50 GeV, this corresponds to the same range: figure 1.2 in fact, is only valid for low P_T jets and the fraction of momentum lost approaches 1/3 for high P_T trackjets. In conclusion, thanks to the higher b-hadron reconstruction efficiency, trackjets are more suitable than calojets for low transverse momentum b-tagging.

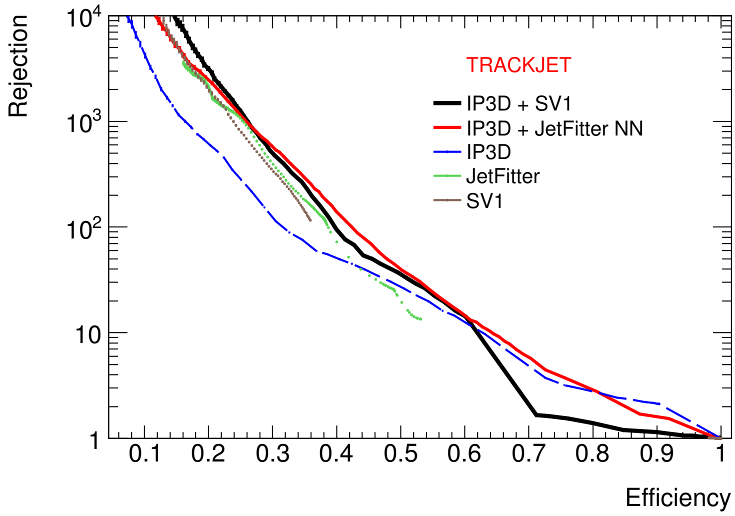

Figure 1.4: Rejection as a function of the tagging efficiency for different ATLAS tagging algorithm tested on trackjets.

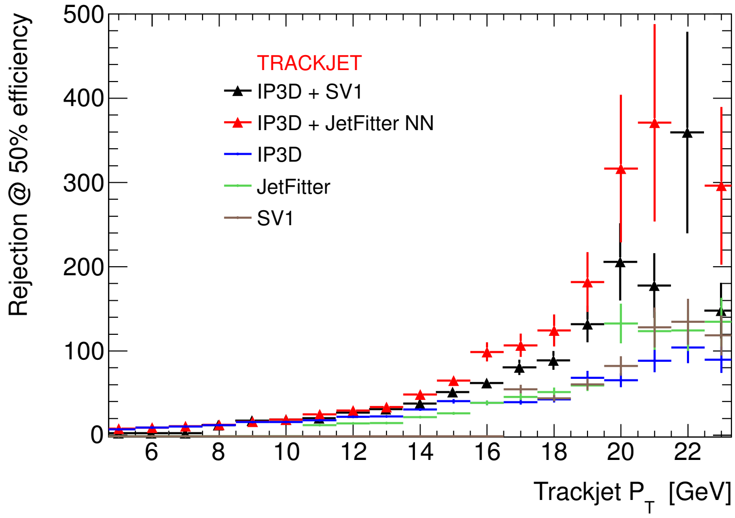

Figure 1.5: Rejection as a function of the transverse momentum of the trackjet for the tagging point which gives 50% tagging efficiency for that P_T value. Different ATLAS tagging algorithm are reported.

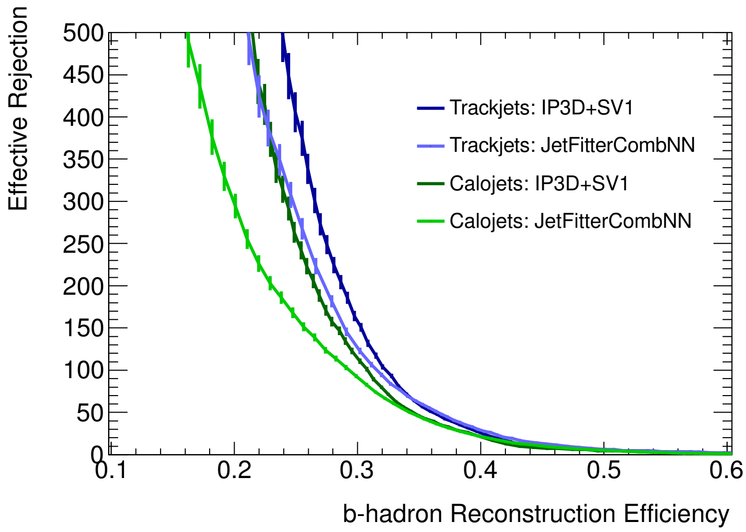

Figure 1.6: Effective rejection as a function of b-hadron reconstruction efficiency, trackjet and calo jets are compared for two different ATLAS tagging algorithms. Trackjets are selected in the transverse momentum range between 4 and 33 GeV, while calojets between 8 and 50 GeV.

1.2.2 Impact of Trackjet on the Analysis

The impact of trackjets on the neutral MSSM Higgs search is tested in a preliminary study and reported in what follows. Preselections[1], as defined in in section **??**, are applied to MC samples of signal and backgrounds with the following exceptions on the definition of taggable jets:

- Calorimeter taggable jets should have $|\eta| < 2.5$ and $20 < P_T < 50$ GeV.
- Track taggable jets should have $|\eta| < 2.5$ and $5 < P_T < 33$ GeV.
- The tagging algorithm used is "IP3D+SV1" at its 70% tagging efficiency point.

the event yields for $bbA/h/H$ production, $Z \rightarrow \tau\tau$ and $t\bar{t}$ (the two most important backgrounds of the b-tag category) are reported in table 1.2 normalized to an integrated luminosity of 1 fb^{-1}. Along with the preselection yields other interesting

[1] This study has not been updated with the newest version of the object reconstruction selections and corrections, a difference of the order of 10% is expected with respect the numbers in table **??**.

Selection	Signal $bbA/H/h$		$Z \to \tau\tau$		$t\bar{t}$	
Preselection	127.2 ± 2.2		3017 ± 8		2066 ± 5	
	Calojet	Trackjet	Calojet	Trackjet	Calojet	Trackjet
At least one taggable jet	47.3 ± 0.8	106.9 ± 1.8	1146 ± 3	2513 ± 7	1804 ± 4	2014 ± 5
Exactly one jet matched b-hadron	18.4 ± 0.3	46.7 ± 0.8	4.5 ± 0.3	18.2 ± 0.5	1054 ± 3	959.1 ± 2.3
Exactly one tagged jet	10.2 ± 0.1	21.0 ± 0.6	37.3 ± 0.5	107 ± 1	777 ± 4	630 ± 4

Table 1.2: Impact of trackjets on the analysis, the event yield is compared between trackjets and calojets. For signal b-associated production is simulated for $\tan\beta = 20$. The yields are normalized to an integrated luminosity of 1 fb^{-1}, all the selections are meant after preselection.

selections are reported, those are X for the characterization of jet and b-tagging impact on the analysis, calojets and trackjets yields are compared for each of them. As expected, after requiring exactly one b-tagged jet, trackjets presents higher efficiency on signal and higher rejection of top background, which is the most important background for the b-tag category. However, lower transverse momentum requirements on trackjets implies higher tagging fake rates, which is seen as an increase of $Z \to \tau\tau$ background, this may be also a serious issue for QCD multi-jet background, even tough this is a minor background in b-tag category.

Concluding, the use of trackjets in the b-tag category is very promising and can bring up to twice better sensitivity[2], however, to exploit the full power of this technique a dedicated b-tagging calibration on trackjets is needed, study on algorithm

[2]Note that this estimate is done according to $s/\sqrt{b}$ ratio, considering a counting experiment without systematic uncertainties and only two backgrounds, it represent then the upper limit to the gain in sensitivity with the current b-tagging performance.

improvements for low P_T b-tagging are also desirable, furthermore, systematics uncertainty on trackjets need to be evaluated. A preliminary study, addressing one of the most important systematics uncertainty for trackjets, is reported in section 1.3.

1.2.3 A Novel Technique for low-P_T b-Tagging

this small paragraph will be added if I manage to access trackjets data on MDTRaid16, I just need to reproduce one plot which is missing.

1.3 Systematic Uncertainties on Trackjets

1.3.1 Introduction to Trackjet Systematics

There are several sources of systematic uncertainties on trackjets that may contribute to physics observables mismodeling, those effects are briefly summarized in what follows, the focus is on energy scale and reconstruction efficiency systematic uncertainties.

Uncertainty can arise from MC generator details, like the particular choice of PDF and fragmentation functions, or details of the parton shower and underlying event, challenging to simulate for low transverse momentum object. Those uncertainty can be evaluated by means of a dedicated MC Rivet [88] analysis, they will be dependent on the specific use of trackjets and need to be evaluated case by case.

Energy scale and resolution for single tracks is found to be very well modeled by simulation for tracks above 500 MeV [92], thus, uncertainty on the energy scale and resolution that arise form mismodeling of the pattern recognition algorithm are considered to be negligible.

In dense track environment different tracks may share same hits and this can generate degradation of resolution, fake tracks, loss of track efficiency. Mismodeling of tracks shared hits may affect in general trackjet energy scale, resolution and reconstruction efficiency. This kind of effects has been checked in [94], where calojet energy scale uncertainty are measured using tracks, it has been shown that effects due to tracks hit merging are negligible for jets with $P_T < 300$ GeV.

Mismodeling of the inner detector material budged leads to track reconstruction efficiency mismodeling, which strongly affects trackjets. A methodology to estimate energy scale and reconstruction efficiency uncertainty on trackjets, due to material budget mismodeling, is presented for the first time in section 1.3.2.

1.3.2 Trackjets Uncertainty from Material Budget

An obvious, but rather inconvenient way, to estimate uncertainty due to inner detector (ID) material budget mismodeling, is to produce the relevant MC samples of a given analysis modifying the ID material budget in them. It can be shown that the primary effect of material budget mismodeling influences mainly track reconstruction efficiency (see section 1.3.3), an alternative approach would be then to modify the track efficiency in a given sample according to its uncertainty [93, 95] and build trackjets out of the new collection of tracks. A tool has been made which randomly removes tracks according to reconstruction efficiency uncertainty, trackjets which are build out of this subset of tracks are called in the following *INEF-trackjets*.

A minimum bias MC simulation sample is reproduced containing standard trackjets and INEF-trackjets. A set of ”isolated” trackjet with cone size $\Delta R = 0.4$ are selected, isolated means that no other trackjet should be reconstructed within a distance of $\Delta R = 1$. INEF-trackjets are then matched with the original trackjet via cone matching in an event by event basis, the matching fails if no INEF-trackjet is found within $\Delta R = 0.8$ from the original one. Result on the deterioration of the trackjets efficiency and of the energy scale are presented respectively in figure 1.7 and 1.8, these results are based on the current knowledge of inner detector material budged [93]. For low transverse momentum trackjets, uncertainty on the material budget translates into an energy scale shift of 2-4% and in a reduction of the mean number of tracks. This method can only simulate excess of material (reduced track efficiency) but not a lack of material (increased track efficiency), however, for the latter case a symmetric effect is expected.

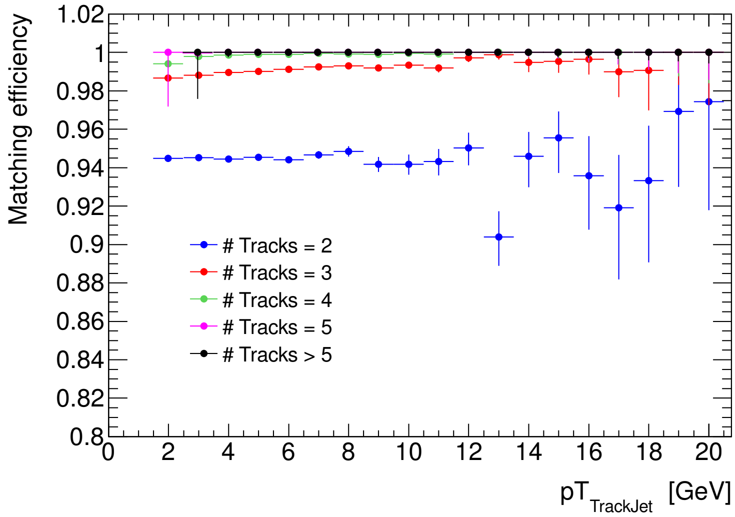

Figure 1.7: INEF-Trackjets are matched with standard trackjets, here is reported the matching efficiency as a function of P_T and number of track of standard trackjet.

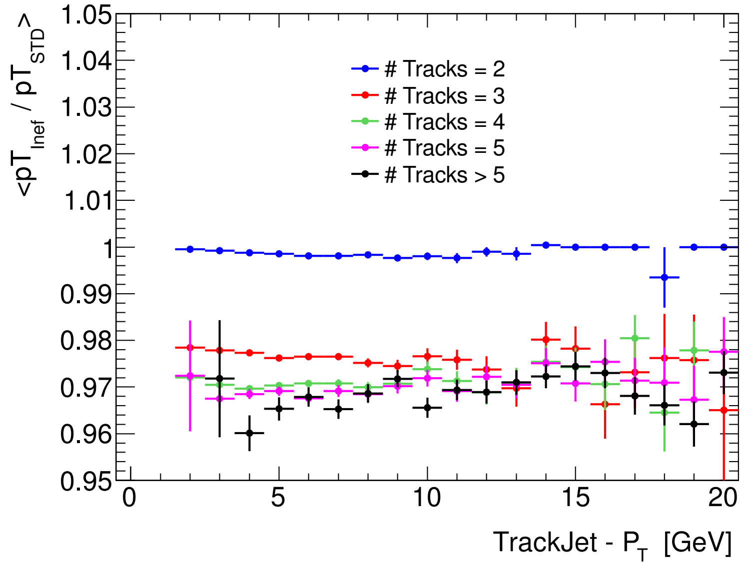

Figure 1.8: INEF-Trackjets are matched with standard trackjets, here is reported the effect on the energy scale as a function of P_T and of the number of tracks of the standard trackjet.

1.3.3 Track Subtraction Method Validation

The method described in section 1.3.2 depends strongly on the assumption that hadronic secondary interaction, within the inner detector, leads manly to lost of tracks and only in a marginal way to a decrease of tracks quality, a consequence is that material budget mismodeling influences mainly track reconstruction efficiency. In this section, effect of material budget uncertainty on tracks resolution and fake rate are evaluated, this is achieved by means of a simulated sample of minimum bias events, where extra material is added to the ID increasing uniformly of 10% the interaction length.

The requirement on tracks are the ones defined in section 1.1, furthermore a track should be matched within $\Delta R < 0.1$ with a stable[3] simulated particle which should be responsible (alone) of at least 80% of the track hits, tracks that do not fulfil these requirements are called fakes. Fake tracks are tracks that come from a random combination of hits generated from different particles. The track fake rate, shown in figure 1.10, is about 1-3%, the extra material sample has a total increase of the track fake rate of permille. Resolution as shown in figure 1.9 is about 1% for large range of tracks P_T, the total increase of resolution in the extra material sample is also of the order of permille. The deterioration of the tracks resolution and fake rate due to extra material is then negligible compared to the one of track reconstruction efficiency, which undergo to a total decrease in the extra material sample of 1-2%, decrease in efficiency has serious impact on trackjet energy scale. Figure 1.11 shows the ratio of the track reconstruction efficiency of primary particle between the standard and extra material sample.

Results from INEF-trackjets (builded in a standard sample) are also directly compared with trackjets from extra material sample, the comparison is done by means of trackjet-to-truthjet matching (see section 1.2 for truthjets matching) and is reported in figure 1.12 and 1.13 for reconstruction efficiency and energy scale respectively. INEF-trackjets shows to reproduce correctly the effect of extra material either on reconstruction efficiency and energy scale, giving, in most of the cases, a

[3]Here is intended a Generator stable and interacting particle, which means a charged particle with decay length greater than 1m, also stable particle from secondary interactions are considered.

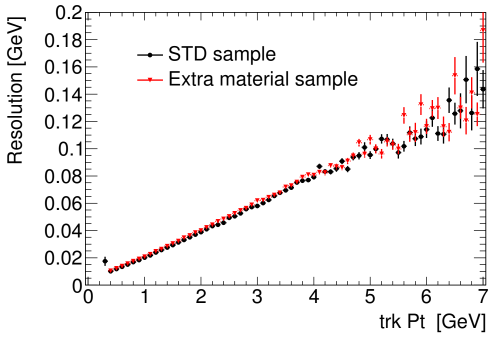

Figure 1.9: Track resolution with respect to matched truth particle as a function of truth particle P_T, for standard Pythia minimum bias sample and 10% inner detector extra material sample.

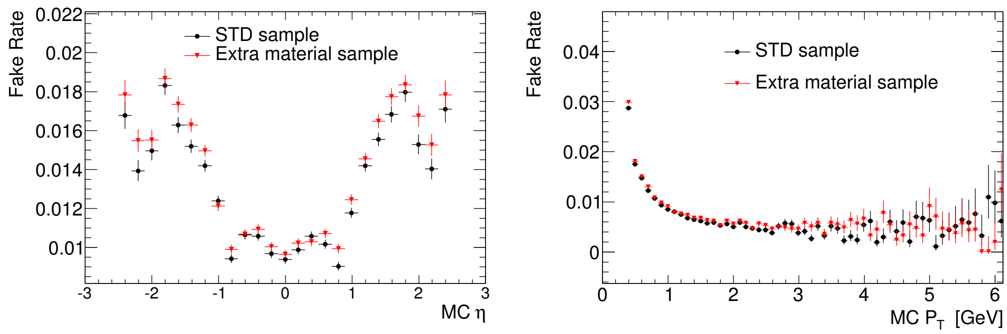

Figure 1.10: Track fake rate resolution as a function of track η (left) and track P_T (right), for standard Pythia minimum bias sample and 10% inner detector extra material sample.

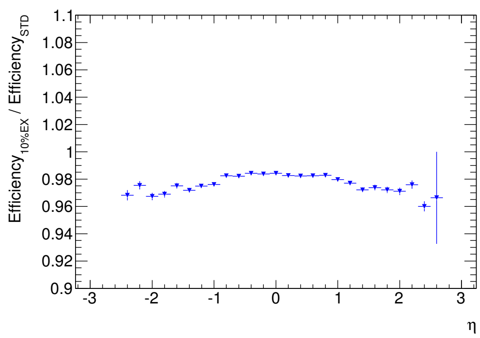

Figure 1.11: Track efficiency with respect to primary truth particle as a function of truth particle η, reported is the ratio between standard Pythia minimum bias sample and 10% inner detector extra material sample.

conservative estimate.

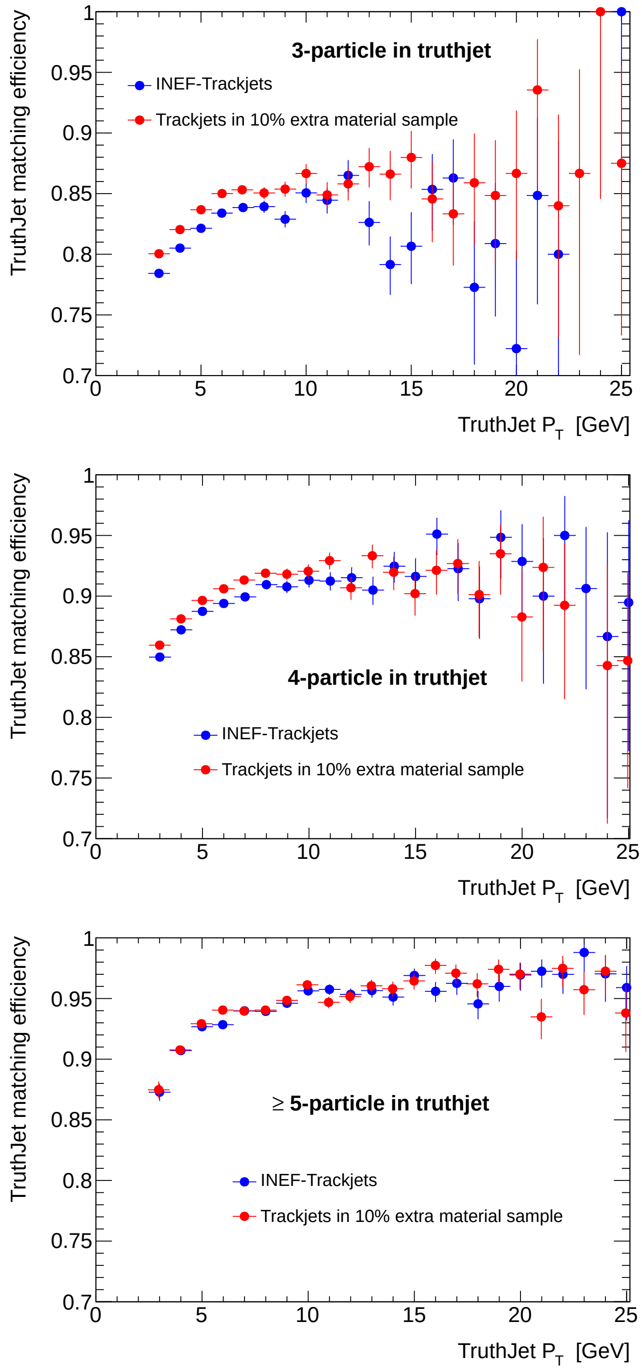

Figure 1.12: Jet reconstruction efficiency with respect to truthjet for INEF-trackjets and trackjets in a 10% extra material sample, in case of 3,4 and ≥ 5 truth-particle. INEF-trackjets always reproduce correctly the inefficiency or give a conservative estimate.

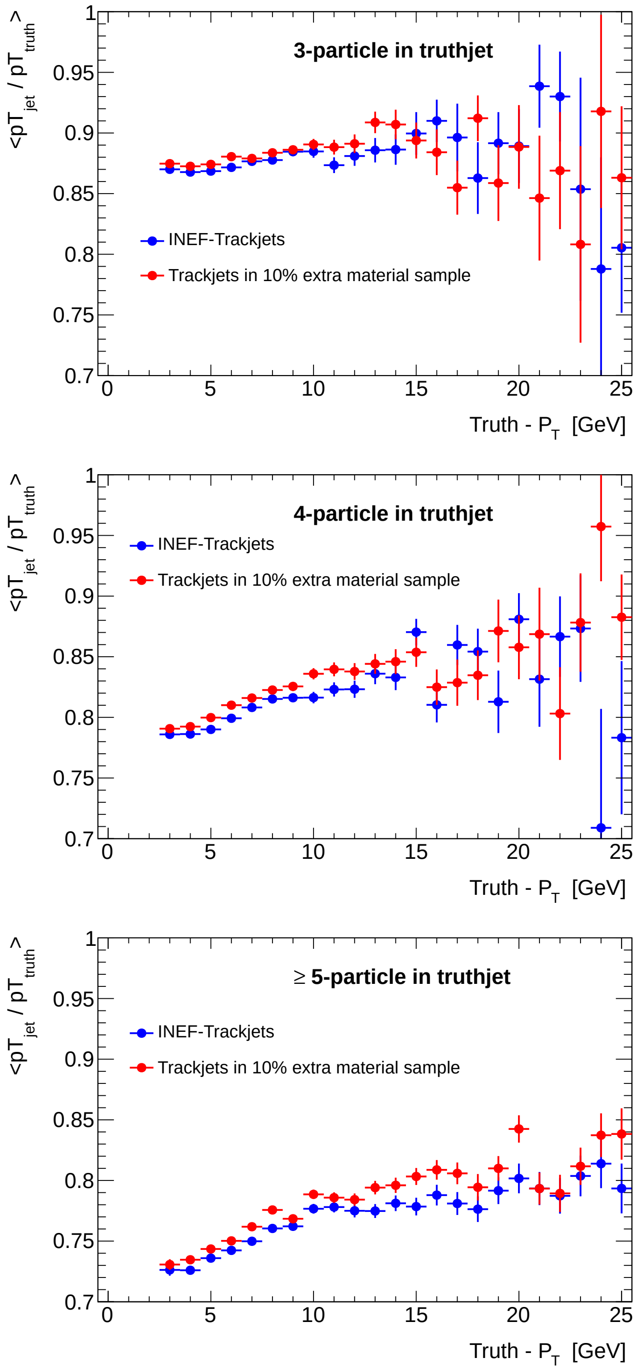

Figure 1.13: Fraction jet transverse momentum with respect to truthjet for INEF-trackjets and trackjets in a 10% extra material sample, in case of 3,4 and ≥ 5 truth-particle. INEF-trackjets always reproduce correctly the inefficiency or give a conservative estimate.

Bibliography

[1] L. Evans and P. Bryant, *LHC Machine*, JINST **3** (2008) S08001.

[2] F. Englert and R. Brout, *Broken Symmetry and the Mass of Gauge Vector Mesons*, Phys. Rev. Lett. **13** (1964) 321.

[3] P. W. Higgs, *Broken symmetries, massless particles and gauge fields*, Phys. Lett. **12** (1964) 132.

[4] P. W. Higgs, *Broken Symmetries and the Masses of Gauge Bosons*, Phys. Rev. Lett. **13** (1964) 508.

[5] P. W. Higgs, *Spontaneous Symmetry Breakdown without Massless Bosons*, Phys. Rev. **145** (1966) 1156.

[6] G. S. Guralnik, C.R. Hagen and T. W. B. Kibble Phys.Rev.Lett. **13** (1964) 585.

[7] N. P. Nilles, *Supersymmetry, supergravity and particle physics*, Phys. Rep. **110** (1984) 1.

[8] H. E. Haber and G. L. Kane, *The search for supersymmetry: Probing physics beyond the standard model*, Phys. Rep. **117** (1985) 75.

[9] ALEPH, DELPHI, L3 and OPAL Collaboration, *Search for neutral MSSM Higgs bosons at LEP*, Eur. Phys. J. **C47** (2006) 547.

[10] *Combined CDF and D0 upper limits on MSSM Higgs boson production in tau-tau final states with up to 2.2 fb^{-1} of data*, `arXiv:1003.3363 [hep-ex]`.

[11] CDF Collaboration, T. Aaltonen et al. Phys. Rev. Lett. **103** (2009) 201801.

[12] D0 Collaboration, V. Abazov et al. Phys. Rev. Lett. **101** (2008) 071804.

[13] TNPWG (Tevatron New Physics Higgs Working Group), CDF and D0 Collaborations, *Search for Neutral Higgs Bosons in Events with Multiple Bottom Quarks at the Tevatron*, `arXiv:1207.2757 [hep-ex]`.

[14] CDF Collaboration, T. Aaltonen et al., *Search for Higgs Bosons Produced in Association with b-quarks*, Phys.Rev. **D85** (2012) 032005, `arXiv:1106.4782 [hep-ex]`.

[15] D0 Collaboration, V.M. Abazov et al., *Search for neutral Higgs bosons in the multi-b-jet topology in 5.2fb^{-1} of $p\bar{p}$ collisions at $\sqrt{s} = 1.96$ TeV*, Phys.Lett. **B698** (2011) 97–104, `arXiv:1011.1931 [hep-ex]`.

[16] The CMS Collaboration, S. Chatrchyan et al., `arXiv:1104.1619 [hep-ex] [hep-ex]`.

[17] The ATLAS Collaboration , *Search for the neutral Higgs bosons of the Minimal Supersymmetric Standard Model in pp collisions at $\sqrt{s} = 7$ TeV with the ATLAS detector*, `arXiv:1211.6956 [hep-ex]`.

[18] T. A. Collaboration, *Observation of a new particle in the search for the Standard Model Higgs boson with the ATLAS detector at the LHC*, Physics Letters B **716** (2012) 1–29.

[19] T. C. Collatoration, *Observation of a new boson at a mass of 125 GeV with the CMS experiment at the LHC*, Physics Letters B **716** (2012) 30–61.

[20] S. Heinemeyer, O. Stål and G. Weiglein, *Interpreting the LHC Higgs search results in the MSSM*, Phys.Lett. **B710** (2012) 201–206, `arXiv:1112.3026 [hep-ph]`.

[21] A. Arbey, M. Battaglia, A. Djouadi and F. Mahmoudi, *The Higgs sector of the phenomenological MSSM in the light of the Higgs boson discovery*, JHEP **1209** (2012) 107, `arXiv:1207.1348 [hep-ph]`.

[22] The ATLAS Collaboration, G. Aad et al., *The ATLAS Experiment at the CERN Large Hadron Collider*, JINST **3** (2008) S08003.

[23] M. L. Mangano et al., *ALPGEN, a generator for hard multiparton processes in hadronic collisions*, JHEP **07** (2003) 001.

[24] J. Alwall et al., *Comparative study of various algorithms for the merging of parton showers and matrix elements in hadronic collisions*, Eur. Phys. J. **C53** (2008) 473, `arXiv:0706.2569`.

[25] S. Frixione and B. R. Webber, *Matching NLO QCD computations and parton shower simulations*, JHEP **06** (2002) 029, `hep-ph/0204244`.

[26] B. P. Kersevan and E. Richter-Was, *The Monte Carlo Event Generator AcerMC 2.0 with Interfaces to PYTHIA 6.2 and HERWIG 6.5*, `arXiv:0405247v1 [hep-ph]`.

[27] G. Corcella et al., *HERWIG 6: an event generator for hadron emission reactions with interfering gluons (including supersymmetric processes)*, JHEP **01** (2001) 010.

[28] J. M. Butterworth, J. R. Forshaw, and M. H. Seymour, *Multiparton Interactions in Photoproduction at HERA*, Z. Phys. **C72** (1996) 637.

[29] T. Binoth, M. Ciccolini, N. Kauer, and M. Kramer, *Gluon-induced W-boson pair production at the LHC*, JHEP **12** (2006) 046.

[30] A. S. et al., *Higgs boson production in gluon fusion*, JHEP **02** (2009) 029.

[31] T. Gleisberg et al., *Event generation with SHERPA 1.1*, JHEP **02** (2009) 007.

[32] J. Pumplin, D. R. Stump, J. Huston, H. L. Lai, P. M. Nadolsky and W. K. Tung, "New generation of parton distributions with uncertainties from global QCD analysis," JHEP **0207** (2002) 012 [hep-ph/0201195].

[33] H. -L. Lai, M. Guzzi, J. Huston, Z. Li, P. M. Nadolsky, J. Pumplin and C. - P. Yuan, "New parton distributions for collider physics," Phys. Rev. D **82** (2010) 074024 [arXiv:1007.2241 [hep-ph]].

[34] S. Heinemeyer *et al.* [LHC Higgs Cross Section Working Group Collaboration], "Handbook of LHC Higgs Cross Sections: 3. Higgs Properties," arXiv:1307.1347 [hep-ph].

[35] M. Carena, S. Heinemeyer, C. E. M. Wagner, and G. Weiglein, *Suggestions for benchmark scenarios for MSSM Higgs boson searches at hadron colliders*, Eur. Phys. J. **C26** (2003) 601–607, `hep-ph/0202167`.

[36] The ATLAS Collaboration, *ATLAS Monte Carlo Tunes for MC09*, ATL-PHYS-PUB-2010-002.

[37] S. Jadach, J. H. Kuhn and Z. Was, *TAUOLA - a library of Monte Carlo programs to simulate decays of polarized τ leptons*, Comput. Phys. Commun. **64** (1990) 275.

[38] E. Barberio, B. V. Eijk and Z. Was, *Photos - a universal Monte Carlo for QED radiative corrections in decays*, Comput. Phys. Commun. **66** (1991) 115.

[39] The GEANT4 Collaboration, S. Agostinelli et al., *GEANT4 - a simulation toolkit*, Nucl. Instrum. Meth. **A506** (2003) 250.

[40] The ATLAS Collaboration, G. Aad et al., *The ATLAS Simulation Infrastructure*, ATLAS-SOFT-2010-01-004, submitted to Eur. Phys. J. C., `arXiv:1005.4568`.

[41] The ATLAS Collaboration, *Estimation of $Z \to \tau\tau$ Background in VBF $H \to \tau\tau$ Searches from $Z \to \mu\mu$ Data using an Embedding Technique*, ATL-PHYS-INT-2009-109.

[42] The ATLAS Collaboration, *Search for the Standard Model Higgs boson in the $H \to \tau\tau$ decay mode with 4.7 $fb1$ of ATLAS detector*, Tech. Rep. ATLAS-CONF-2012-014, CERN, Geneva, Mar, 2012.

[43] The ATLAS Collaboration, *Search for the Standard Model Higgs boson $H \to \tau\tau$ decays with the ATLAS detector*, ATL-COM-PHYS-2013-722.

[44] T. S. et al., Z *physics at LEP 1*, CERN 89-08 **3** (1989) 143.

[45] A. Bazan, T. Bouedo, P. Ghez, M. Marino and C. Tull, “The Athena data dictionary and description language,” eConf C **0303241** (2003) MOJT010 [cs/0305049 [cs-se]].

[46] The ATLAS Collaboration, Inner Detector: Technical Design Report, CERN/LHCC/97-016/017 (1997).

[47] The ATLAS Collaboration, G. Aad et al., The ATLAS Experiment at the CERN Large Hardon Collider, 2008 JINST 3 S08003.

[48] T. Cornelissen et al., Concepts, Design and Implementation of the ATLAS New Tracking, ATLAS Note ATL-SOFT-PUB-2007-007 (2007).

[49] Kalman, R. E. (1960). *”A New Approach to Linear Filtering and Prediction Problems”.* Journal of Basic Engineering 82 (1): 3545. doi:10.1115/1.3662552

[50] The ATLAS Collaboration, *Characterization of Interaction-Point Beam Parameters Using the pp Event-Vertex Distribution Reconstructed in the ATLAS Detector at the LHC*, ATL-CONF-2010-027.

[51] R. Fruhwirth, W. Waltenberger, P. Vanlaer, *Adaptive vertex fitting*, J. Phys. G34 (2007).

[52] The ATLAS Collaboration, Performance of primary vertex reconstruction in proton-proton collisions at $s = sqrt(7)$ TeV in the ATLAS experiment. ATLAS-CONF-2010-069.

[53] The ATLAS Collaboration, *Expected Performance of the ATLAS Experiment - Detector, Trigger and Physics*, CERN-OPEN-2008-020, `arXiv:0901.0512`.

[54] M. Cacciari, G. P. Salam, and G. Soyez, *FastJet user manual*, Eur.Phys.J. C72 (2012) 1896.

[55] W. Lampl et al., *Calorimeter Clustering Algorithms : Description and Performance*, ATL-LARG-PUB-2008-002.

[56] E. Abat, J. Abdallah, T. Addy, P. Adragna, et al., *Combined performance studies for electrons at the 2004 ATLAS combined test-beam*, JINST 5 (2010) P11006.

[57] ATLAS Collaboration, *Jet energy measurement with the ATLAS detector in proton-proton collisions at* $\sqrt{s} = 7$ *TeV*, Submitted to EPJ (2011) , arXiv:1112.6426

[58] The ATLAS Collaboration, *Pile-up corrections for jets from proton-proton collisions at ATLAS in 2011*, ATLAS-CONF-2012-064, July, 2012.

[59] M. Cacciari and G. P. Salam, *Pileup subtraction using jet areas*, Phys.Lett. B659 (2008) 119.

[60] The ATLAS Collaboration, G. Aad et al., *Jet energy resolution in proton-proton collisions at* $\sqrt{s} = 7$ *TeV recorded in 2010 with the ATLAS detector*, Eur.Phys.J. C73 (2013) 2306

[61] The ATLAS collaboration, *Jet energy scale and its systematic uncertainty in proton-proton collisions at* $\sqrt{s} = 7$ *TeV with ATLAS 2011 data*, ATLAS-CONF-2013-004

[62] T. Barillari et al., *Local Hadron Calibration*, ATL-LARG-PUB-2009-001.

[63] The ATLAS Collaboration, *Jet energy scale and its systematic uncertainty in proton-proton collisions at* $\sqrt{s} = 7$ *TeV in ATLAS 2010 data*, ATLAS-CONF-2011-032.

[64] M. Cacciari, G. P. Salam, and G. Soyez, *The anti-kt jet clustering algorithm*, JHEP 04 (2008) 63.

[65] G. Piacquadio, C. Weiser, *A new inclusive secondary vertex algorithm for b-jet tagging in ATLAS*, JPCS 119 (2008) 032032

[66] The ATLAS Collaboration, G. Aad et al., *Commissioning of the ATLAS high-performance b-tagging algorithms in the 7 TeV collision data, ATLAS-CONF-2011-102*, CERN, 2011, ATLAS-CONF-2011-102.

[67] The ATLAS Collaboration, *ATLAS Muon Momentum Resolution in the First Pass Reconstruction of the 2010 p-p Collision Data at* $\sqrt{s} = 7\ TeV$, ATLAS-CONF-2011-046.

[68] The ATLAS Collaboration, *Muon reconstruction efficiency in reprocessed 2010 LHC p-p collision data recorded with the ATLAS detector*, ATLAS-CONF-2011-063.

[69] The ATLAS Collaboration, *Expected electron performance in the ATLAS experiment*, ATLAS-PUB-2011-006.

[70] ATLAS egamma WG, *Electron efficiency measurements*, https://twiki.cern.ch/twiki/bin/view/AtlasProtected/EfficiencyMeasurements.

[71] M. Cacciari, G. P. Salam, and G. Soyez, *The anti-*k_t *jet clustering algorithm*, JHEP **04** (2008) 063.

[72] TheATLAS Collaboration, *Performance of the Reconstruction and Identification of Hadronic tau Decays in ATLAS with 2011 Data*, ATLAS-CONF-2012-142.

[73] The ATLAS Collaboration, *Reconstruction and Calibration of Missing Transverse Energy and Performance in Z and W events in ATLAS Proton-Proton Collisions at* $\sqrt{s}$=7 TeV, ATLAS-CONF-2011-080.

[74] A. Elagin, P. Murat, A. Pranko, and A. Safonov, *A New Mass Reconstruction Technique for Resonances Decaying to di-tau*, `arXiv:1012.4686 [hep-ex]`. * Temporary entry *.

[75] ATLAS Jet/EtMiss Combined Performance Group, *Jet Energy Resolution Provider*, https://twiki.cern.ch/twiki/bin/view/Main/JetEnergyResolutionProvider.

[76] The ATLAS Collaboration, *Data-Quality Requirements and Event Cleaning for Jets and Missing Transverse Energy Reconstruction with the ATLAS Detector in Proton-Proton Collisions at a Center-of-Mass Energy of* $\sqrt{s} = 7\ TeV$, ATLAS-CONF-2010-038.

[77] T. A. Collaboration, *Search for neutral MSSM Higgs bosons decaying to* $\tau\tau$ *pairs in proton-proton collisions at with the ATLAS detector*, Physics Letters B **705** (2011) no. 3, 174 – 192.

[78] The ATLAS Collaboration, *Data-driven estimation of the background to charged Higgs boson searches using hadronically-decaying tau final states in ATLAS,* ATLAS-CONF-2011-051.

[79] The ATLAS Collaboration, *Measurement of the* $Z \to \tau\tau$ *cross section with the ATLAS detector*, Phys. Rev. D **84** (2011) 112006.

[80] T. A. Collaboration, *Search for the neutral Higgs bosons of the Minimal Supersymmetric Standard Model in pp collisions at* $\sqrt{s} = 7$ *TeV with the ATLAS detector*, JHEP , `arXiv:1211.6956`.

[81] Atlas statistics forum, *ABCD method in searches*, link

[82] The ATLAS Collaboration, *Search for Neutral MSSM Higgs Bosons H to* $\tau\tau$ *to* $l\tau_h$ *with the ATLAS Detector in 7 TeV Collisions*, ATL-COM-PHYS-2012-094.

[83] The ATLAS Collaboration, *Search for neutral Higgs Bosons in the decay mode* $H \to \tau\tau \to ll{+}4\nu$ *in proton proton collision at* $\sqrt{7}$ *TeV with the ATLAS Detector*, ATL-COM-PHYS-2011-758.

[84] The ATLAS Collaboration, *Measuring the b-tag efficiency in a ttbar sample with 4.7* fb^{-1} *of data from the ATLAS detector* ATLAS-CONF-2012-097.

[85] The ATLAS Collaboration, *Calibration of b-tagging using dileptonic top pair events in a combinatorial likelihood approach with the ATLAS experiment* ATLAS-CONF-2014-004.

[86] The ATLAS Collaboration, *Luminosity Determination in pp Collisions at* $\sqrt{s} = 7$ *TeV using the ATLAS Detector in 2011*, ATLAS-CONF-2011-116.

[87] T. Sjostrand, S. Mrenna and P. Skands, *PYTHIA 6.4 physics and manual*, JHEP **05** (2006) 026.

[88] A. B. et al., *Rivet user manual*, `arXiv:1003.0694 [hep-ph]`.

[89] E. G. G. Cowan, K. Cranmer and O. Vitells, *Asymptotic formulae for likelihood-based tests of new physics*, `arXiv:1007.1727 [hep-ex]`.

[90] LHC Higgs Cross Section Working Group, S. Dittmaier, C. Mariotti, G. Passarino, R. Tanaka (Eds.), et al., *Handbook of LHC Higgs Cross Sections: 1. Inclusive Observables*, `arXiv:1101.0593 [hep-ph]`.

[91] LHC Higgs Cross Section Working Group, S. Dittmaier, C. Mariotti, G. Passarino, and R. Tanaka (Eds.), *Handbook of LHC Higgs Cross Sections: 2. Differential Distributions*, CERN-2012-002 (CERN, Geneva, 2012) , `arXiv:1201.3084 [hep-ph]`.

[92] ATLAS collaboration *Performance of the ATLAS Silicon Pattern Recognition Algorithm in Data and Simulation at* $\sqrt{s} = 7$ *TeV*, ATLAS-CONF-2010-072

[93] The ATLAS Collaboration, *A measurement of the material in the ATLAS inner detector using secondary hadronic interactions*, arXiv:1110.6191, JINST 7 (2012) P01013

[94] The ATLAS Collaboration, *Validation of the ATLAS jet energy scale uncertainties using tracks in proton-proton collision* $\sqrt{s} = 7$ *TeV*, ATLAS-CONF-2011-067

[95] The ATLAS Collaboration, *Track Reconstruction Efficiency in* $\sqrt{s} = 7$ *TeV Data for Tracks with* $P_T > 100$ *MeV* , ATL-PHYS-INT-2010-112

[96] D. de Florian, G. Ferrera, M. Grazzini and D. Tommasini, *Transverse-momentum resummation: Higgs boson production at the Tevatron and the LHC*, JHEP **1111** (2011) , `arXiv:1109.2109 [hep-ph]`.

[97] Statistical twiki, NuissanceCheck. https://twiki.cern.ch/twiki/bin/view/AtlasProtected/Nuisan